Assessing the Tropical South Atlantic atmosphere thermodynamics under distinct Sea Surface Temperature patterns

Thiago L. V. Silva (thiago.luiz.lx@gmail.com)
Agência Pernambucana de Águas e Clima https://orcid.org/0000-0001-5326-4622
Doris Veleda
Federal University Of Pernambuco
Alexandre Costa
Federal University Of Pernambuco
Claudia Parise
Federal University of Maranhão
Rita Alves
Federal University of Rio Grande do Sul
Pedro Tyaquica
Federal University of Pernambuco
Francis Lopes
Federal University of Pernambuco
Leo Aroucha
Federal University of Pernambuco

Research Article

Keywords: rainfall, ocean environment, Southern Atlantic Warm Pool (SAWP)

Posted Date: June 21st, 2021

DOI: https://doi.org/10.21203/rs.3.rs-561512/v1

Assessing the Tropical South Atlantic atmosphere thermodynamics under distinct Sea Surface Temperature patterns

Thiago L. V. Silva, Doris Veleda, Alexandre Costa, Claudia K. Parise, Rita C. M. Alves, Pedro Tyaquiçã, Francis Lopes, Léo Aroucha.

Affiliations

Thiago Silva: Pernambuco Water and Climate Agency (APAC), Av. Cruz Cabugá, Recife, Pernambuco, Brazil. Center for Renewable Energy from the Federal University Of Pernambuco (CER/UFPE), Recife, Pernambuco, Brazil. Tel.: +55 (81) 9999427277. E-mail: thiago.luiz.lx@gmail.com.

Doris Veleda: Department of Oceanography (DOCEAN) and, Center for Renewable Energy from the Federal University Of Pernambuco (CER/UFPE), Recife, Pernambuco, Brazil E-mail: doris.veleda@ufpe.br

Alexandre Costa: Renewable Center for Renewable Energy from the Federal University Of Pernambuco (CER/UFPE), Recife, Pernambuco, Brazil E-mail: alexandre.acosta@ufpe.br

Claudia K. Parise: Laboratory for Climate Studies and Modeling, Department of Oceanography and Limnology, Federal University of Maranhão, Portuguese Ave. 1966, 65080-805 São Luis, Brazil.
E-mail: claudiakparise@gmail.com

Rita C. M. Alves: State Center for Remote Sensingand Meteorology Research, Federal University of Rio Grande do Sul CEPSRM/UFRGS,Porto Alegre, Brazil. E-mail: rita.cma@terra.com.br

Pedro Tyaquiçã: Department of Oceanography (Docean) and Center for Renewable Energy from the Federal University of Pernambuco (CER/UFPE), Recife, Pernambuco, Brazil. E-mail: tyaquica@gmail.com

Francis Lopes: Department of Oceanography (Docean) and, Center for Renewable Energy from the Federal University of Pernambuco (CER/UFPE), Recife, Pernambuco, Brazil. E-mail: fslopes89@gmail.com

Léo Aroucha: Department of Oceanography (Docean) and, Center for Renewable Energy from the Federal University of Pernambuco (CER/UFPE), Recife, Pernambuco, Brazil. E-mail: leo_aroucha@hotmail.com

Corresponding Author

Correspondence to Thiago Silva.

Abstract Northeast Brazil (NEB) is a susceptible region to the occurrence of extreme rainfall events. Sea surface temperature (SST) is used as an indicator for predicting intense weather events in this region. The westernmost Tropical South Atlantic region, also called Southern Atlantic Warm Pool (SAWP), is characterized by a source of heat and humidity which creates atmospheric instability for the NEB. In June 2010 the eastern coast of NEB (ENEB)was influenced by heavy rainfall, causing flash floods and landslides. On the other hand, 2012 marked the beginning of a period of droughts that affected the whole NEB area. The SAWP temperature in turn recorded anomalous values of + 1ºC (-0.5ºC) in 2010 (2012), respectively, although in June 2012 intense rainfall was recorded in ENEB, even with intense negative SST anomalies. With the Coupled-Ocean-Atmosphere-Wave and Sediment Transport (COAWST) model, simulations were made to characterize 2010 and 2012 atmospheric conditions, modifying the SST input data in both situations. The goal of this work is to assess the meteorological systems that occurred in 2010 and 2012 using observational, reanalysis, and simulated data, as well as to identify changes in atmospheric instability patterns, which are under influences of different SST conditions. We performed four cases, including: a) SST measured in 2010 with 2010 atmospheric conditions; b) SST measured in 2012 with weather conditions of 2010; c) SST measured in 2012 with 2012 weather conditions; d) measured in2010 with atmospheric conditions from 2012. The results showed that SAWP temperature significantly influenced the instability of meteorological systems. The impacts were more significant in the lower layer of the

atmosphere, especially in the variables that lead to low-level instabilities. Also, it was observed that warmer atmospheric conditions favor the ocean environment to remain warmer, maintaining the unstable conditions over SAWP.

1 Introduction

Northeast Brazil (NEB) presents a pronounced space-time rainfall variability as a result of atmospheric forcings (Rao et al. 1993; Hastenrath 2012; Hänsel et al. 2016; Correia Filho et al. 2019). Since the Colonial Era, in the 16th century, the NEB is recording migration from inland to coastal areas due to droughts occurred mainly in semiarid regions (Marengo et al. 2017). Meanwhile, severe rainfall in coastal areas can lead to flash floods and landslides with deaths and economic losses, mostly due to uneven urban space organization, and the occupation of hills or slopes, which favors geological instability(Gomes et al. 2012; Dos Santos et al. 2018).

The semiarid, which corresponds to an area of about 1,542,000 km2 or ~11% of Brazil, is the region most vulnerable to droughts and desertification in the NEB(Marengo et al. 2017; Carvalho et al. 2020). In contrast, the Eastern and Northern Northeast Brazilian (ENEB and NNEB) coasts have not only a high susceptibility to intense rainfall episodes, landslides, flash floods, sea-rising damages, but also the most significant number of inhabitants in NEB(Hounsou-gbo et al. 2015; Neves et al. 2016; Debortoli et al. 2017; Rodrigues et al. 2020).

The rainfall variability in the NEB northern and central semiarid regions is associated with the Inter-Tropical Convergence Zone (ITCZ) north-south migration (Moscati and Gan 2007; Rodrigues et al. 2011; Hastenrath 2012; Marengo et al. 2017). In the southern, western, and central regions of the NEB, the South Atlantic Convergence Zone (SACZ) variability contributes to the semiarid region's rainfall events during austral spring and summer (Paegle and Mo 2002). In January and February, Upper Troposphere Cyclonic Vortices (UTCVs) are present (Fereira and Melo 2005). In the eastern NEB (ENEB), the precipitation is modulated by Easterly Waves Disturbances (EWD) (Ramos 1975; Torres and Ferreira 2011; Kouadio et al. 2012; Gomes et al. 2015) with maximum rainfall between May and July, and annual average precipitation above 1500 mm. The Sea Surface Temperature (SST) anomalies over Tropical South Atlantic (TSA) and El Niño Southern Oscillation (ENSO) that interact with global circulation cause climatic variability in the NEB region (Moura and Shukla 1981; Andreoli and Kayano 2006, 2007; Silva and Guedes 2012; Silva et al. 2018; Moura et al. 2020).

In the westernmost TSA region, also known as Southern Atlantic Warm Pool (SAWP), the SST is well correlated with the NEB precipitations (Moura et al. 2009), and is connected to water vapor transport from ocean to the land (Cavalcanti et al. 2002), and heat and moisture exchange between ocean and atmosphere (Foltz and McPhaden 2006; Cintra et al. 2015; Hounsou-gbo et al. 2015; Silva et al. 2018). The dynamic associated with warm water is the decreasing stability through enhanced vertical mixing by large eddies that deepen the boundary layer and reduce momentum from the upper boundary layer (Chelton and Xie 2010). Also, the warm pool can generate more (less) variability of precipitation when the SST anomaly has more (less) spatial variability (Wang et al. 2006).

The interaction between air and sea is essential for understanding the climatic variability due to heat, momentum, and moisture exchange (Bourras et al. 2004). The Marine Atmosphere Boundary Layer (MABL) vertical structure is a crucial factor for triggering the occurrence of synoptic activities such as deep convection (Peng et al. 2016). Ocean surface fluxes are determined by SST and near-surface air temperature, humidity, and wind speed, all of which explicitly are linked to the MABL processes (Zeng et al. 2004). The warmer (colder) and larger (smaller) warm pool areas are connected to more (less) intense formation of hurricanes in the North Atlantic(Wang et al. 2006). Therefore, the SAWP is an essential region to enhance meteorological systems over ENEB, leading to variability and severe rainfall episodes(Silva et al. 2018).

Considering the adverse conditions for housing, financial inequality, and economic dependence on the local climate, the NEB becomes a place with potential vulnerability due to climate change and variability (Hastenrath 2012). Climate changes are expected to cause significant human impacts on the ENEB population, from a visual change on the coast(Costa et al. 2010), to social-economic consequences (Hastenrath 2012), including also an increase in health issues like Dengue, Zika, and Chikungunya virus (Ebi and Nealon 2016), and vulnerabilities which imply in increased social inequality and more significant damage to ENEB society.

SST anomaly is one of the most relevant indicators of quantifying global and regional climate change (Bojinski et al. 2014). Due to the strong influences of SAWP on the ENEB intense rainfall (Cintra et al. 2015; Hounsou-gbo et al. 2015; Silva et al. 2018), it is essential to understand how climate variations in the South Atlantic SST can lead the rainfall variability at the ENEB region. June of both 2010 and 2012 were characterized

by easterly waves over the SAWP region, but with different rainfall variability. In 2010, persistent SST anomaly up to 1ºC records preceded extreme rainfall events at ENEB. On the other hand, in 2012, negative SST anomalies were commonly recorded in the Tropical South Atlantic and were the beginning of the most prolonged periods of drought in the NEB (Silva and Guedes 2012; Marengo et al. 2017). The drought event affected regions which were not commonly affected by this severe rainfall deficit, such as ENEB.

Due to the lack of observational data, and the need for environmental management, civil defense and strategic planning, terrestrial system models fill this gap. The ocean-atmosphere coupled models allow high-frequency turbulence and radiative exchange processes between the model's components with a defined small time-step. Hypothesis tests enable us to identify climatic patterns that might influence future climates. These adverse weather scenarios should serve as a resource for urban planning to mitigate the effects of natural disasters and minimize social impacts in a situation of potential climate change.

We performed simulations with Weather Research and Forecasting (WRF) and the Regional Oceanic Model System (ROMS) in a two-way coupled model with Coupled Ocean-Atmosphere-Wave and Sediment Transport (COAWST) modeling system (Warner et al. 2008, 2010; Renault et al. 2012). The experiments consisted of changing the SST input data in the model, making the SST an independent variable for these simulations. We performed four cases, including i) SST measured in 2010 with 2010 atmospheric conditions; ii) SST measured in 2012 with weather conditions of 2010; iii) SST measured in 2012 with 2012 weather conditions; iv) SST measured in2010 with atmospheric conditions from 2012.

The objective of this work is to evaluate the 2010 and 2012 meteorological events in the ENEB under different SST anomalies over the SAWP region, simulating the possible impact of the SAWP on the extreme rainfall at the ENEB, regarding climate change scenarios.

2 Methods

The study area (50ºW - 20ºW; 20ºS - 5ºN) covers part of the Western South Tropical Atlantic, including the South Atlantic Warm Pool (SAWP, 34ºW - 25ºW; 12.5ºS - 4ºS) as well as the Eastern Northeast Brazil(ENEB, 40.5ºW - 35ºW; 15.5ºS - 4ºS). Figure 1 shows the topography and bathymetry of the simulation domain.

a. Observational Dataset

We used satellite images from Geostationary Operational Environmental Satellite (GOES) from the National Oceanic and Atmospheric Administration (NOAA) and Meteosat from European Organization for the Exploitation of Meteorological Satellites (EUMETSAT). Atmospheric sounding profiles for Recife - PE, Salvador – BA, Natal - RN and Fernando de Noronha -PE from the Wyoming University (Figure 1, white dots); Precipitation data from the *Agência Pernambucana de Águas e Clima* (APAC) (Figure 1, yellow dots), the *Agência Executiva Gestão das Águas da Paraíba* (AESA) (Figure 1, purple dots), and the *Empresa de Pesquisa Agrícola do Rio Grande do Norte* (EMPARN) (Figure 1, blue dots).

We performed trends in the number of rainy days in precipitation intervals for the states' capitals located in the ENEB following Greene et al. (2019), being: i) Prec. Event <1mm; ii) 1 mm <Prec. Event <30 mm; iii) 30 mm <Prec. Event <100 mm; iv) Prec. Event> 100 mm. The dataset consists of daily observed rainfall from 1979 to 2019, and was provided by INMET.

Radiosonde data from the University of Wyoming database was collected for both weather events at specific points in the ENEB. The goal is to investigate atmospheric instability during the period of the highest intensity of the meteorological systems. Thus, the radiossonde data collected for this analysis were: Fernando de Noronha (ref. SBFN: -3.85 Lat; -32.41Lon), Recife (ref. 82900: -8.05 Lat; -34.91 Lon), and Salvador (ref. 83229: -13.02 Lat; -36.52 Lon) for 2010, and Natal (ref. SBNT: -5.91 Lat; -35.15 Lon) for 2012. The change of this last point was due to the absence of radiosonde on that specific day.

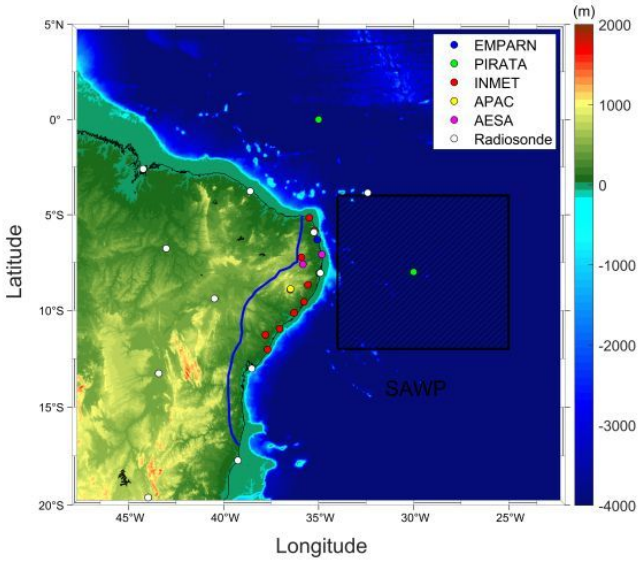

FIG. 1. Study area. Crosshatched square is the South Atlantic Warm Pool (SAWP) region. Colored dots are weather stations coming from various state meteorological agencies and ocean buoys. Dark Blue (EMPARN), Green (PIRATA Buoys), Red (INMET), Yellow (APAC), Purple (AESA), and White are the positions of radiosondes (Wyoming University).

b. Reanalysis and Regional Modeling

In order to determine the precipitation response of the ENEB region to SAWP SSTs, we used precipitation data from the Climate Prediction Center (CPC) Global Unified Gauge-Based Analysis of Daily Precipitation (Xie et al. 2007) in the period from 1979 to 2019, as well as data from the NOAA Extended Reconstructed SST V5 (Huang et al. 2017)for the same period. We performed treatment for daily precipitation, selecting case events according to the day with or without rainfall and the intervals recorded similar to ENEB state's capital. After the registered event filter, we applied the sum of annual cases, totaling the annual rainfall number of events. After treatment, daily rainfall, as well as SST over the Tropical South Atlantic trends were performed, based on the algorithms of Greene et al. (2019), indicating the trends for spatial rainfall episode in NEB and Western Tropical Atlantic SST trends for the period 1979-2019.

For the WRF component, the initial and boundary conditions were from the NCEP Final Operational Global Analysis Data (FNL)(NCEP 2000), with a horizontal resolution of 1.0° x 1.0°. For the ROMS model, the variables of temperature, salinity, and currents (*u, v*) for the oceanic model were given by the Hybrid Coordinate Ocean Model (HYCOM), with a horizontal resolution of 0.08° x 0.08° (Wallcraft et al. 2008).

The coupled model domain consists of the 42 vertical levels in ETA coordinates in the atmospheric model and 30 ETA levels in the oceanic model, the last one with depth up to 1000m. The domain consists of 240 points distributed in longitude and 242 points in latitude, with 12 km of resolution for the WRF model. The ROMS model is 200 points in longitude, 202 in latitude, and 12 km resolution.

We performed four coupled modeling experiments, with different SST input data for two years of different climate conditions, 2010 and 2012:

i. 2010 run with SST of 2010: SST for 10 June 2010 and all atmospheric and oceanic conditions for this period;
ii. 2010 run with SST of 2012: same meteorological and oceanic conditions of 2010, except the SST, which is for 10 June 2012, when the average SST of the region was colder than 2010;
iii. 2012 run with SST of 2012: SST for 10 June 2012 and all atmospheric and oceanic conditions for this period;
iv. 2012 run with SST of 2010: same meteorological and oceanic conditions of 2012, except the SST, which is for 10 June 2010, when the average SST of the region was warmer than 2012.

We performed simulations for the period between 05/17/2010 to 06/19/2010 and 05/21/2012 to 06/20/2012. The simulations were configured with Atmosphere and Ocean models activated exchanging information every 10 minutes of time-steps.

c. Climate Projection Dataset

The climate projections data are from the fifth and sixth phase of the Coupled Model Intercomparison Project (CMIP5 and CMIP6) on the World Climate Research Program (WCRP) platform. It used the Representative Concentration Pathways (RCP) 4.5 for climate scenario, corresponding to the radiative forces of +4.5 $W.m^{-2}$ until the end of the 21st century, as well as several climatic models consisting of boundary conditions (r), physical of the model (i) as well as disturbances in the initial state of the data (p). The same was valid for CMIP6, using the SSP245 experiment, an update of RCP4.5 project. The variables used consisted of projected SST, as well as monthly precipitation, using climatology for (a) 2020 to 2040, (b) 2040 to 2070, and (c) 2070 to 2100, from SAWP area as well as from ENEB area.

The analysis in this work was performed analysis from CMIP5 and CMIP6 multi-model experiments. It performed collections of the simulated values and the respective intervals of maximum and minimum of the simulations, leading to an analysis of the probable scenario. The chosen experiment for projections characterizes the "middle of the road," that is, a scenario that is neither as optimistic nor pessimistic.

3 Results

a. Climate Overview

The ENEB is a narrow coastal strip that differsin terms of biome and annual total rainfall from the neighbor semiarid areas of the NEB. The predominant characteristic of ENEB region is the milder climate, with smaller thermal amplitudes (on average) and a growing topography towards the continent, besides holding the most populous municipalities located in the coastal areas.The maximum precipitation occurs in June, duringthe rainy season, between April and July, mainly due to the easterly waves disturbances. The rainy season is well correlated with high SST in the SAWP region with a lag of approximately three months, as seen in Figure 2.

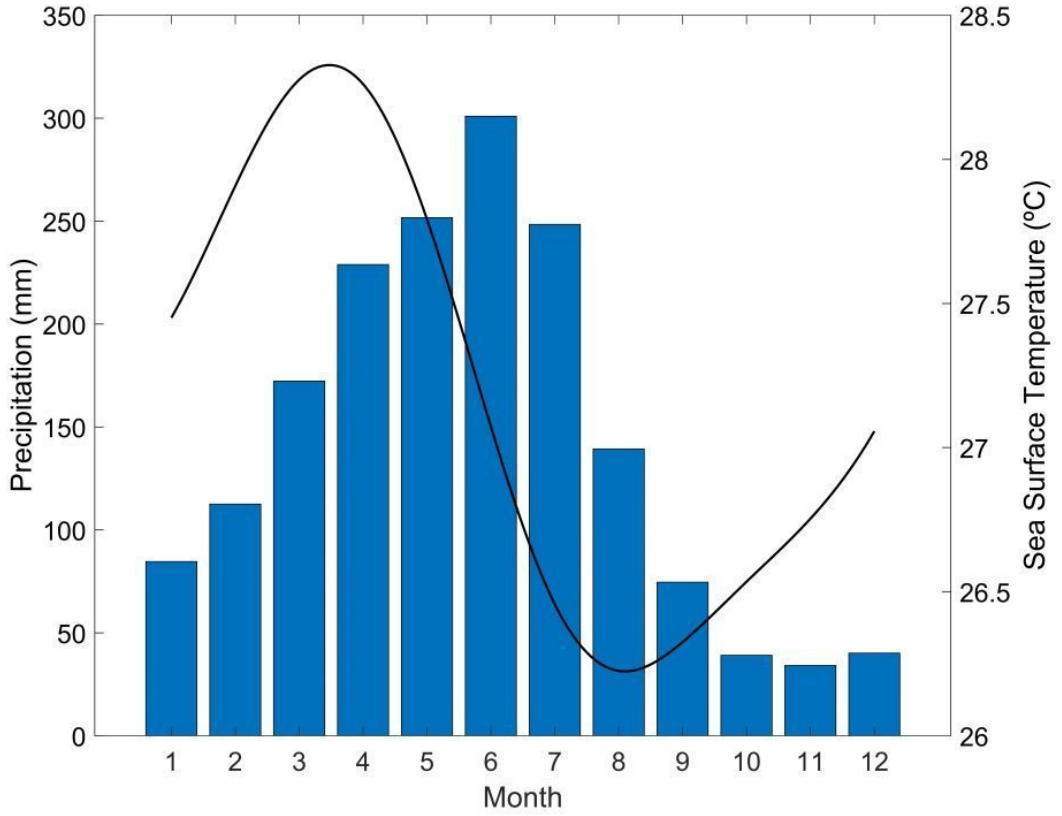

FIG. 2. Monthly accumulated rainfall climatology from 1979 to 2019for ENEB averaged area (bar) and mean monthly sea surface temperature climatology over SAWP region (lines).

The rainfall regime in the ENEB responds to the SST both in the Atlantic and Pacific oceans (Moura and Shukla 1981; Andreoli and Kayano 2006, 2007; Silva and Guedes 2012; Silva et al. 2018; Moura et al. 2020). The release of latent heat, water vapor transport, and moisture convergence ispositively correlated tothe rainfall regime of the ENEB (Foltz and McPhaden 2006). The most important meteorological systems in the period, such as the EWD and disturbances in the trade winds, also respond directly to the SST patterns (Moura et al. 2009; Silva et al. 2018).

The definition of warm pools considers SST values exceeding 28.5ºC in the near closed oceanic region, weak trade winds, resultant deep convection, and has a distinct seasonal cycle (Wang et al. 2006). The SST climatology for the SAWP region shows that such values occur predominantly in March. However, in positively anomaly years, the SAWP may appear months before and vanish months later (e.g., 2010 and 2011 years), in the same way, in negatively years, the SAWP may not even be characterized, as between 2012 and 2018 years.

The SAWP has an important influence on the meteorological events that occur in the region. During meteorological events susceptible to rain, the warm pools intensifythe latent heat flow, buoyancy and instabilities at low levels, which increases the probability of extreme events.

Figure 3 shows the coherence in wavelet between SAWP Area SST and the total monthly ENEB rainfall. The results show a high lagged coherence in all years in the period between 8 to 16 months. Also, in the period near to 32 months, we record a high coherence between 1990 to 1996 and 2007 to 2012. The result shown by the wavelets coherence indicates the lagged linear relationship between SST and the region's precipitations. With this, it can project that the increase in SST intensity in this area could lead to more significant volumes of rainfall in coastal regions in the ENEB.

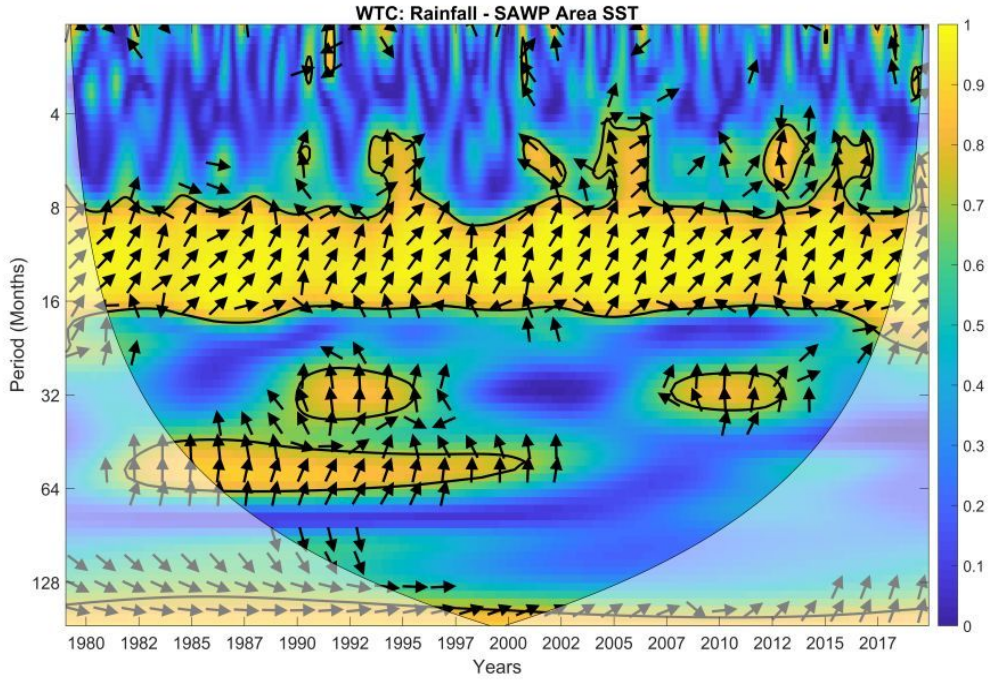

FIG. 3. Wavelet coherence between SST over the SAWP Area and the monthly accumulated precipitation from 1979 to 2019.

Figure 4 shows, on a normalized scale, the trend of daily precipitation events at different intervals. Figure 4a shows an increase daily trends without rainfall for all state capitals in the ENEB. However, the occurrence of rainfall events of intervals between 1 and 30 mm.day^{-1} and from 30 to 100 mm.day^{-1}, in general, are decreased, except for Natal, where rainfall events above 30mm.dia^{-1} increased. For rainfall above 100mm.day^{-1}, there is an increase in the capitals at north of the ENEB (Natal, João Pessoa, and Recife) and a decrease in Sergipe, Salvador and Maceió (Figure 4d).

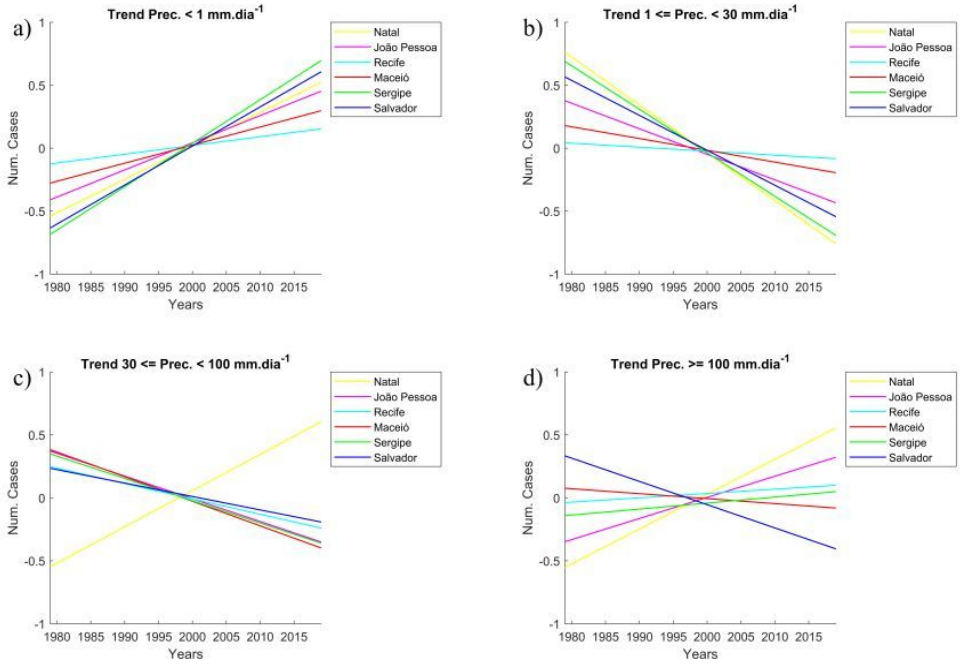

FIG. 4. Normalized trends for: days without rainfall (a), rainfall between 1mm to 30mm (b), rainfall between 30mm to 100mm (c), and above 100mm (d). The lines represent the rainfall trends for ENEB state capitals, from INMET rainfall gauges from 1979 to 2019.

Figure 5 shows the spatial trend of daily NEB rainfall based on GCPC dataset (1979 – 2019). Several regions have showed trends of increasing rainfall above 30mm.day^{-1} and 100 mm.day^{-1}. These results agree with previous results, which showed more significant periods with a lack of rainfall and increasing intense rainfall events in Northeastern Brazil, corroborating with climate projections (Alves et al. 2021).

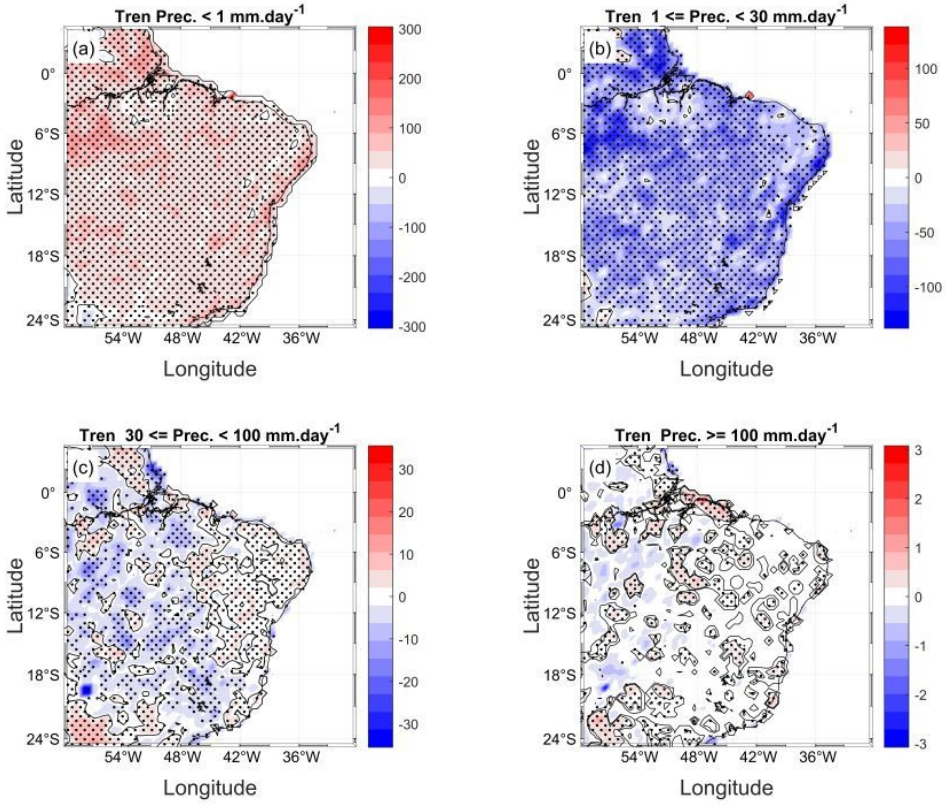

FIG. 5. Spatial trends for: days without rainfall (a), daily rainfall between 1mm to 30mm (b), daily rainfall between 30mm to 100mm (c), and above 100mm. The data was provided by Global Daily Unified Gauge-Based Analysis of Precipitation Project from 1979 to 2019. The contour lines represent the neutral trend, showing the transition between positive trend (red) and negative trend (blue). Positive (negative) trend means that quantity of days, with precipitation in a specific threshold, are increasing (decreasing). The dotted area is the 95% significance.

Similarly, Figure 6 shows the spatial trend of SST anomaly in the WTA, using monthly data from NOAA V3 reanalysis, 2° x 2° of spatial resolution. The northernmost WTA region is warming, with a rate of 0.03ºC per year, from 1979 to 2019. However, the region over the southern branch of the South Equatorial Current (sSEC) has a cooling trend up to 0.05ºC. The SST trends show systematic warming of the regions adjacent to the coast of the NEB, including the SAWP region, which is favorable to more intense precipitation regime and extreme events at the ENEB.

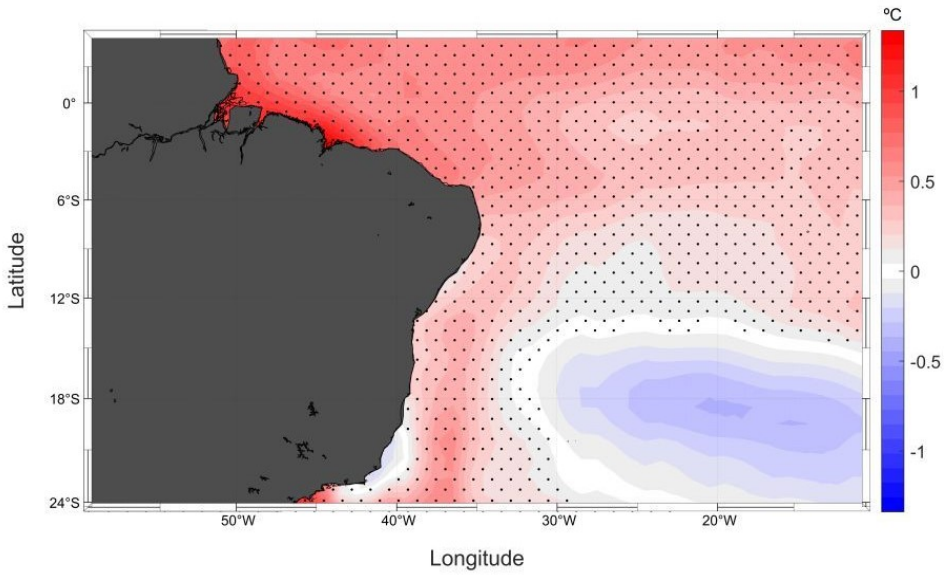

FIG. 6. Sea surface temperature trends in the Western Tropical South Atlantic. The period comprehend data from 1979 to 2019 and the trend is the total for period. The dotted area is the 95% significance.

The analysis for RCP4.5 and SSP245 projections shows a significant increase in the SAWP SSTs for the next decades (Figure 7). The SST until 2040 will increase above 28.5ºC remaining throughout the year. Over the decades, the values of 28.5ºC have continually exceed the threshold, having only averaged values below in the decade from 2040 to 2070, during the austral winter. In the decades from 2070 to 2100, even the minimum threshold exceeds the values of 28.5º in the SAWP Area. Therefore, the climatic characteristics of the STA must undergo a significant change directly influencing the ENEB rainfall climatology.

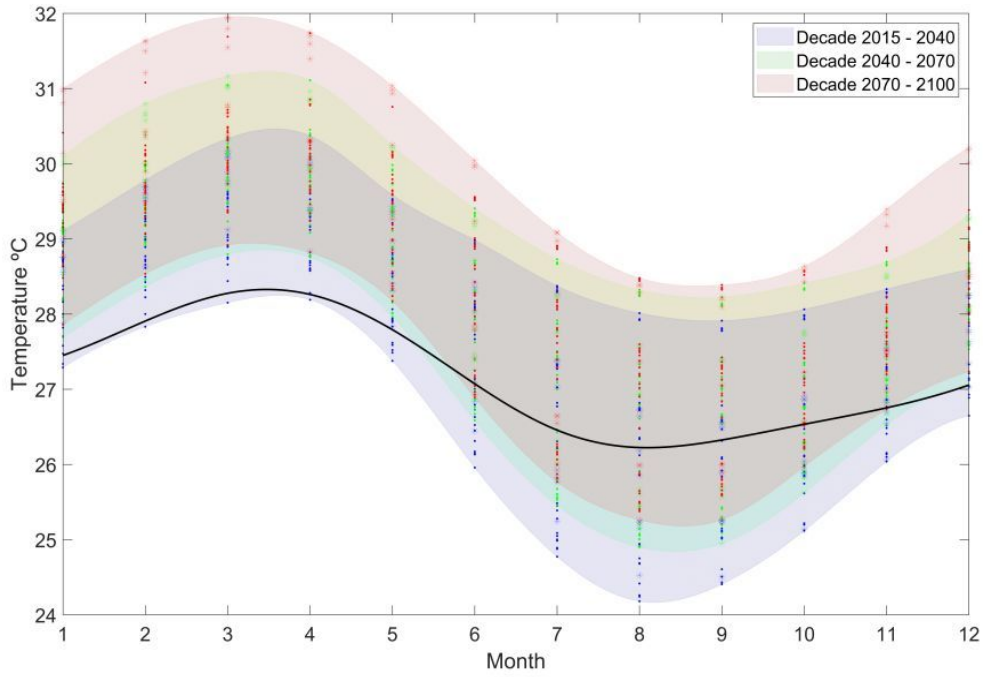

FIG. 7. Projections by CMIP5 (rcp4.5) and CMPI6 (ssp245) experiments sea surface temperature over SAWP area in near future (present-2040) in blue shaded; SAWP projected SST for 2040 to 2070 (green); SAWP projected SST for 2070 – 2100 in red. Black lines are the SST in SAWP area climatology between 1979-2019.

b. Synoptic conditions for the 2010 and 2012 events

Figure 8 shows the initial SST conditions and streamlines at 850 hPa for coupled simulations of four different cases of: SST of 2010 and atmosphere of 2010 conditions (Figure 8a); SST from 2012 and atmosphere from 2010 (Figure 8b); SST of 2012 and atmosphere of 2012 (Figure 8c); SST of 2010 and atmosphere of 2012 (Figure 8d). Data show that the SAWP area recorded higher temperatures in 2010 than in 2012. Also, 2012 doesn't show the 28.5ºC isotherm, indicating the absence of the SAWP region by the criteria of Wang et al. (2006). The 2010 SST, with positive anomalies about 1ºC, is equivalent to the temperatures for the decade of 2020 to 2040; which means, the COAWST simulations with SAWP can represent a real specific scenario of climate change that might be already influencing us.

In 2010 (Figure 8a), there was a southeast wind flow with a magnitude of about 15 $m.s^{-1}$ over the near ocean coast, presenting slight disturbances at 850 hPa. At 700 hPa (Figure 8c), a trough is observed over the SAWP region, indicating a wave disturbance that moved from the ocean towards the continent. Then, at 500 hPa (Figure 8e), the high-intensity eastward flow was associated with a pre-existing post-frontal high pressure, leading to a large amount of water vapor transport also in middle levels of the atmosphere.

In counterpart, in 2012, it was observed southeastern disturbances with weaker winds magnitudes at 850 hPa (Figure 8b). At 700 hPa (Figure 8d), a ridge was present in the southern of NEB with weaker winds. Meanwhile, at 500 hPa (Figure 8f), the southern part of a high pressure favored the trapping of moisture at low levels. It is important highlight that 2012 disturbances had smaller upward motion than in 2010.

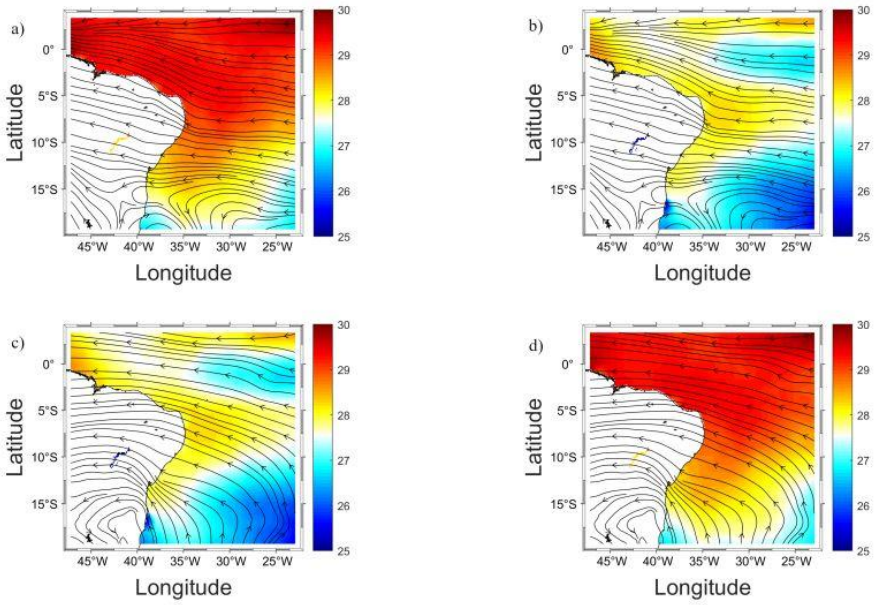

FIG. 8. Initial data from simulations. (a) Initial SST conditions for 2010 and current lines at 850hPa for 2010. (b) Initial SST conditions for 2010 with 2010 atmosphere. (c) Initial SST conditions and 2012 atmosphere. (d) Initial Atmospheric Conditions 2012 with SST2010. It shows that the initial atmospheric dynamics remain the same, both in 2010 and 2012, leaving the SST as an independent variable.

The meteorological systems occurred in 2010 and 2012 had similar wave disturbances in atmosphere low-levels. The simulated period comprised the months with the highest accumulated rainfall for ENEB (May and June). The EWDs are the weather systems with the largest impact on rainfall accumulation in the region during austral winter (Ramos 1975; Torres and Ferreira 2011; Gomes 2012; Kouadio et al. 2012). During 2010, the meteorological event between June 17th and 18th presented low-level instabilities, reaching 700 hPa, and a high pressure in the South Atlantic, which favored the strong easterly winds in 500 hPa. This circulation pattern favors the transport of water vapor from adjacent regions of the Southern Tropical Atlantic to the continent (Cavalcanti et al. 2002), supporting atmospheric convections (Brown and Zhang 1997). However, on June 14th, 2012, the atmosphere showed disturbances at low-levels, but a low wind magnitude with a ridge circulation at 700 hPa, while at 500 hPa an eastward flow, showing water vapor transport from the continent to the ocean (Cavalcanti et al. 2002).

The results from radiosondes showed dry atmospheric conditions from mid to high layers. However, there were high humidity patterns at the Fernando de Noronha and Recife surroundings in 2010, with strong subsidence in Salvador, the southernmost ENEB locality. This pattern shows that the weather system was restricted in the northernmost part of ENEB. The radiosonde for Fernando de Noronha shows a wet layer from the surface near to 700 hPa level, as well as in Recife.

For 2012 radiosondes, the results showed the presence of a significant amount of humidity restricted to the 800 hPa level for Fernando de Noronha and Natal (located between Recife and Fernando de Noronha). However, in Recife, there was a similar characteristic compared to 2010, with low humidity at 700 hPa and a moisten layer above 700hPa and 600 hPa.

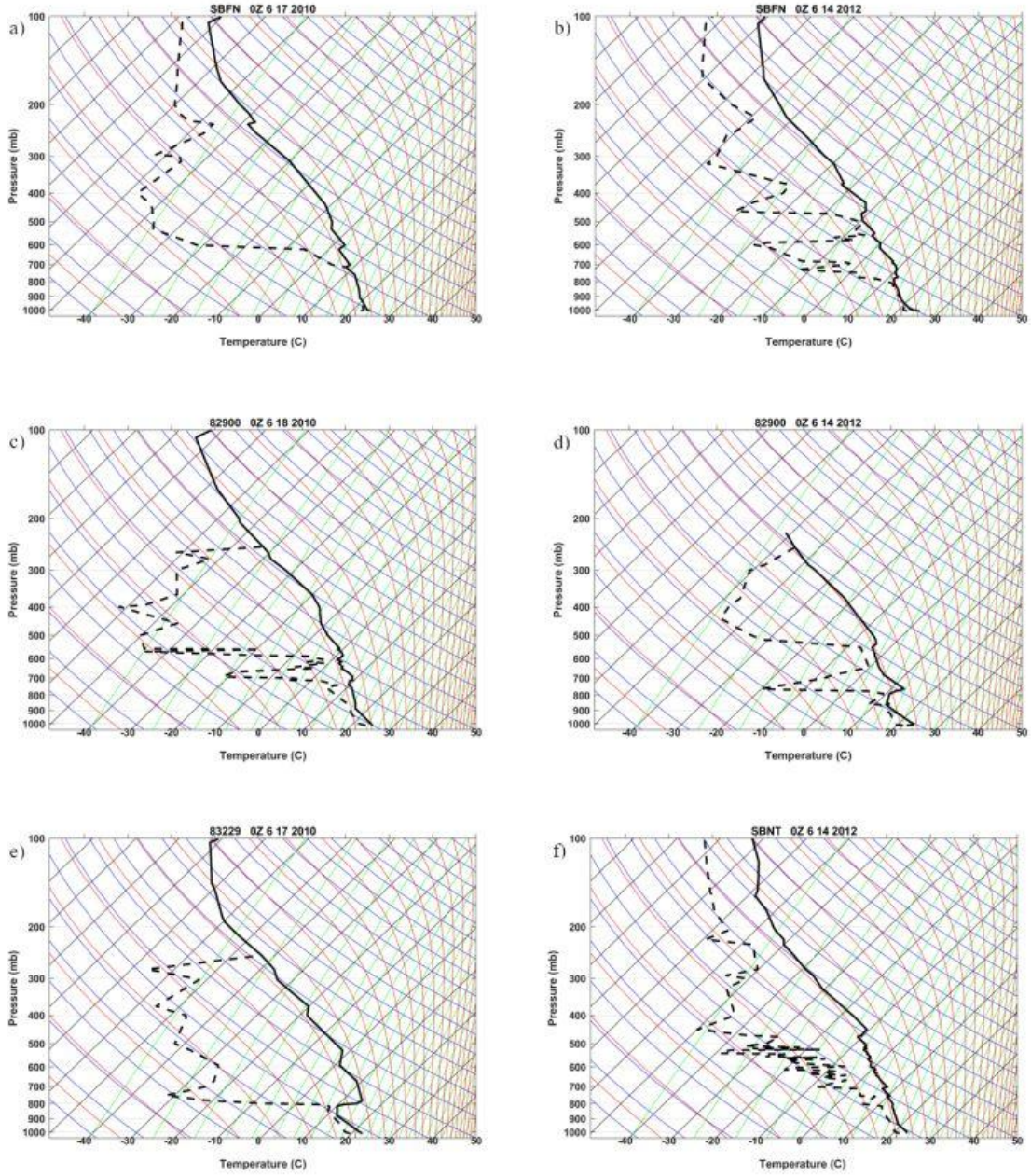

FIG. 9. Radiosonde from Northeastern Brazil during the 2010 and 2012 events. (a) Fernando de Noronha radiosondeat12Z on 17/06/2010. (b) Radiosonde of Fernando de Noronhaat12Z on 06/14/2012. (c) Radiosonde of Recife on 06/18/2010 at 12Z. (d) Radiosonde of Recife at 12Z on 14/06/2012. (e) Radiosonde for Salvador at12Z on 06/10/2010. (f) Radiosonde for Natal at12Z on 09/14/2012.

The instability index values coming from the radiosonde at 06/17/2010 12Z measurements allow the comparison of the probability for atmospheric conditions for deep convection. In 2010, the values indicated median K index values, as well as CAPE and Total Totals Index values, but a large amount of precipitable water mainly in Fernando de Noronha and Recife. It is noteworthy that the radiosonde shown is that recorded on the 17

June at 12Z, while the most substantial convection occurred on the 18th at 00Z, which may underestimate the index values.

In 2012, there are low values of all instability indices, but a large amount of precipitable water, near to 2010 measured, except for Fernando de Noronha which presented a difference of 8mm between 2010 and 2012. Radiosonde measurements for 14 June 2012 coincide with the period of more activity weather systems, showing the atmospheric conditions during the event.

When comparingthe instability indices between the years studied, it is observed that the values in 2010 presented higher intensification for convective buoyancy than in the 2012 event. Thus, the phenomena differs in the cloud formation characteristics, lying deep convective clouds in 2010 (Figure 10a) and shallow convection (Figure 10b) according to the GOES satellite image.

Figure 10a shows the GOES IR satellite images with cloud top temperature enhancement, where the colder values show intense vertical cloud development due to the weather system. It is justified by the high mid-level's atmosphere instability, a through configuration at 700 hPa and a large amount of water vapor transport to the region due to the high-intensity wind speed from ocean to land.

However, Figure 10b shows that there was no intense vertical development. The pattern of satellite images with grey tones of clouds indicate less convection activity than the 2010 weather system. It distinguishes from the instability indices, which were lower in 2012, as well as the precipitable water and water vapor transport, as the winds were less intense, including a ridge at 700 hPa and a eastward flow at 500hPa. Although the characteristics of warm convective clouds, in the event of 2012 the precipitation reached the level of 100 mm.day^{-1} in isolated areas of the Metropolitan Recife Region.

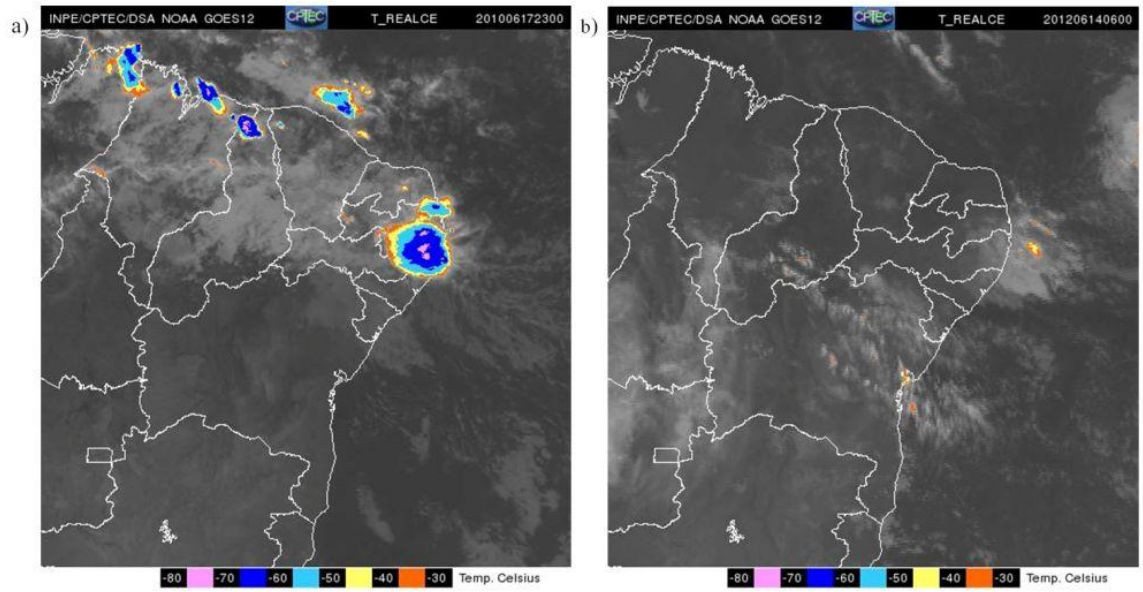

FIG. 10. Satellite images from GOES (Geostationary Operational Environmental Satellite) handled by the National Institute for Space Research (INPE) on (a) 17/06/2010 at 2300Z and (b) 14/06/2012 at 0600Z. The grey scale shows clouds with temperature less than -30ºC. Above this temperature the top cloud is shaded with colors in the bottom of figure.

The radiosonde data complemented the analysis by showing the profiles of the atmosphere during the systems. Atmospheric instabilities associated with the June 2010 event had higher values than June 2012, indicating an increased probability of occurrence of convective events in the region. The atmospheric instabilities in 2010 culminated in an intense convective event with large vertical development that can be seen in satellite imagery. Temperature enhancement at the top of the cloud indicates the presence of a mesoscale convective system acting during the peak of the meteorological system's development. However, according to the synoptic analyzes and radiosonde measurements, cloud development over the period of June 14th, 2012 had no intense convective activities. Cloud characteristics indicate the development of shallow cumulus clouds with slightly

colder small cores. However, warm rainfall (Liu and Zipser 2009) were observed in ENEB mainly in Recife weather stations, which record values close to 100 mm.day^{-1}.

c. Simulations of the 2010 and 2012 Events

An average over the SAWP Area (34ºW - 25ºW; 12.5ºS - 4ºS) was performed to calculate the difference between SST and air temperature at 2m (T_{2m}) (Figure 11a,b). Positive gradient values indicate heat losses from the ocean to the atmosphere. The results (simulations for 2010 atmospheric conditions - Figure 11a) show sea-air gradients oscillating between 0.5ºC and 1ºC with higher gradient values with the 2010 SST. Under 2012 (Figure 11b) weather conditions, and with 2010 SST as input data, high gradient values are predominant.

Figure 11c,d shows the latent heat flux simulations over the SAWP Area. The difference in 2010 (Figure 11c) indicates that the simulations with the SST of the corresponding time presented higher values of latent heat flux compared to those simulated with the 2012 SST. For the 2012 simulation, Figure 11d, it presented higher values with 2010 SST compared to the 2012 values. However, there was a more significant discrepancy in the first moments of the simulations, where the difference between simulations reached 50 W.m^{-2}, whereas, at the end of the simulation, this difference dropped to 10 W.m^{-2}.

The warm pools are either created or vanished according to atmospheric characteristics. A dry and cold atmosphere over a warm SST, for example, is associated with increased latent heat flux from ocean to atmosphere, generating the decease of the warm pool. The opposite occurs in a wet and warm atmosphere, when the latent heat flux losses through evaporation are weakened, and the warm pool intensifies. Hence, process as cloudiness, convective activity and outgoing longwave radiation, are important factor for warm pool formation, maintenance and demise (Wang and Enfield 2003; Clement et al. 2005).

The warm SST maintenance is associated with the warmer and wetter troposphere, reducing not only sea level pressure (SLP) and weaker easterly winds, but also lowering vertical shear and weakening subsidence in the air. During years with a well-developed warm pool, these conditions lead to wetter summers in the Intra American Sea (IAS), Central America (Wang and Enfield 2003) and rainfall regimes in the Western Pacific (Brown and Zhang 1997)**.** The opposite also occurred (Brown and Zhang 1997; Wang and Enfield 2003), with cold water generating dry summers in these regions.

The cooling pattern of the TSA western basin is due to latent heat losses (Foltz and McPhaden 2006) and coincides with the highest rainfall period at ENEB (Cintra et al. 2015), which are also directly related to rainfall anomalies in these areas (Moura and Shukla 1981; Rao et al. 1993; Aragão 1998; Andreoli and Kayano 2006, 2007; Moura et al. 2009; Silva and Guedes 2012; Silva et al. 2018).

Figure 11e,f shows the averaged atmospheric surface pressure for the SAWP Area. The simulated surface pressure presented different patterns, responding to different SST inputs (2010 and 2012). Figure 11e shows the surface pressure for 2010 simulations. The results evidence a lower average surface pressure at beginning of the simulation periods with an increasing from the middle to the end of simulations. In the period with activity of the meteorological system (16 June 2010), the surface pressure decreased. In 2012 (Figure 11f) the surface pressure showed a pattern with weaker variability, and a decreasing surface pressure between 10th and 15th June. Comparing 2010 with 2012, the lower pressure preceeded the rainfall events over ENEB. Also, the simulations shows slightly low values when using high SST input.

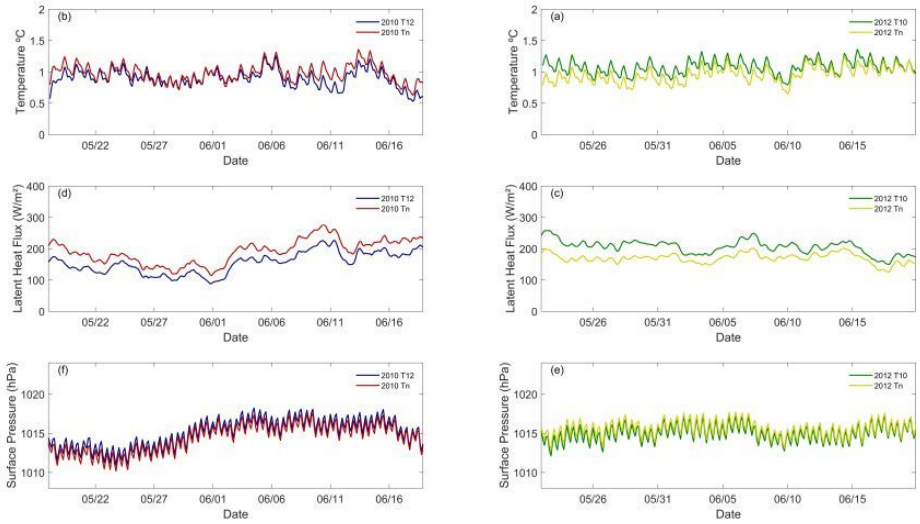

FIG.11. Time-series of: Difference between SST and T_{2m} (air temperature at 2m)for 2010 (a) and for 2012 (b); Latent Heat Flux for 2010 (c) and 2012 (d); Surface Pressure for 2010 (e) and 2012 (f). The values represent the average of SAWP area during COAWST simulations in period from05/17/2010 to 06/19/2010, blue (2010 with SST 2012), red (2010 with SST of the season); 05/21/2012 to 06/20/2012, green (2012 with SST of 2010), yellow (2012 with SST of the time);

The ENEB virtual temperature profile (Figure 12a,b) were plotted to identify MABL thermal instabilities during both weather events (18 June 2010 and 14 June 2012). The results showed warmer MABL when holding the 2010 SST as a boundary condition. Differently, cold SST conditions simulated a small warming of the lower vertical profile. Thus, under high SST conditions, the lower troposphere increases buoyancy at low levels.

Figure 12c,d shows the vertical motions based on omega for the case studies. Omega (ω) represents the rate of change of pressure in a parcel over time (dp/dt), which is proportional to the vertical motion under hydrostatic balance. There were upward movements for all simulations in low-mid levels. The highest values were at low levels up to around 850 hPa for all scenarios. However, the most intense upward movement occurred when the model had the 2010 SST as input. It is noteworthy that, at medium-high levels, the vertical movements were close to zero. However, the simulation of 2012 under the SST of 2010 as boundary conditions, gived rise to upward movements throughout the atmosphere.

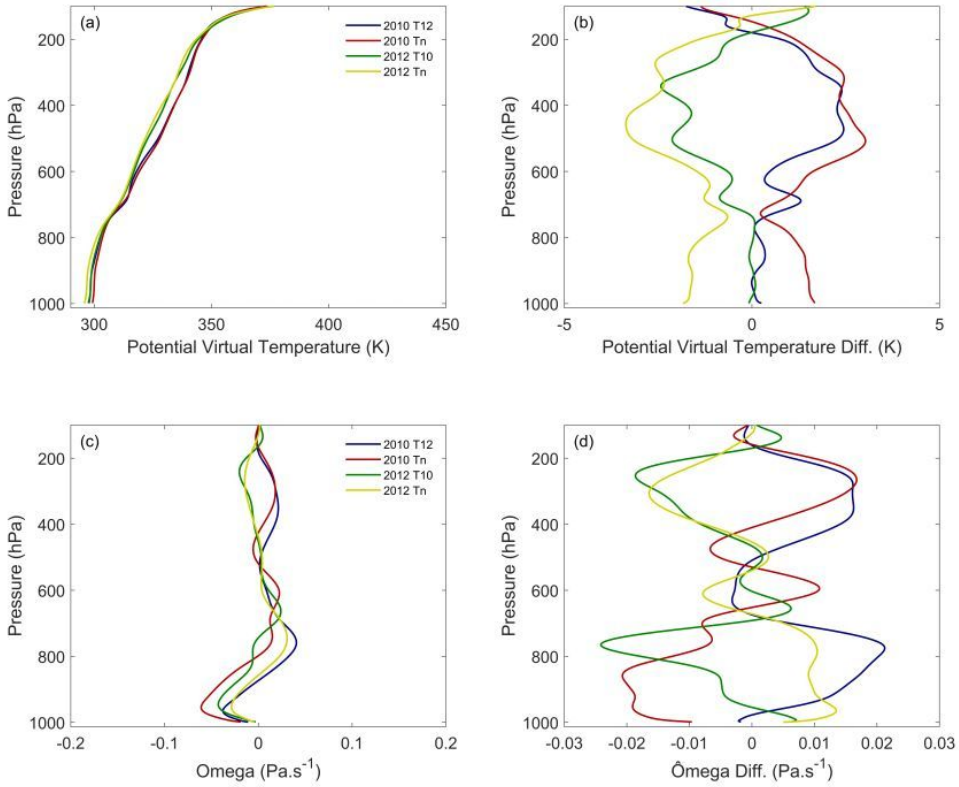

FIG. 12. Vertical profile of Potential Virtual Temperature during peak activity (a) and difference between Potential Virtual Temperature of the experiment minus the average of Potential Virtual Temperature during peak of activity (b); (c) and (d) is the same but for Omega vertical velocity. The period of simulations is for June 2010 and 14 June 2012. The experiments are atmosphere for 2010 with SST with 2012 (blue); atmosphere for 2010 and SST for 2010 (red); atmosphere for 2012 and SST for 2010 (green); atmosphere for 2012 and SST for 2012 (yellow).

The zonal and meridional water vapor transport over ENEB shows the moisture convergence from the ocean. When observing the zonal transport (Figure 13a), it is possible to identify a displacement from east to west at low-mid levels, with higher intensity of around 850 hPa for simulations of both 2010 and 2012 atmosphere conditions. However, the most significant transport occurred in 2010 with higher SST, without any considerable alteration for both simulations of 2012 patterns. The meridional water vapor transport (Figure 13b) showed higher values in lower layers of the atmosphere. In the simulations of 2010, a slight increase in the vapor transport with the SST of 2012 could be verified. However, meridional transport values had a significant increase over warmer SST. The result indicates that in 2012, the highest water vapor transport contribution was from the southernmost regions of the Atlantic, which means the higher SST in the south contributed to the increase of moisture in the ENEB.

The water vapor content in the atmospheric layer is considerably increased in simulations with warmer SSTs (Figure 13c). The vapor content in the ENEB region has a close relationship with the moisture transport from the South Atlantic, where warmest waters favored the increase or the water vapor content. Both 2010 runned simulations presented higher water vapor content than the 2012 simulations (Figure 13d). This is a response to the higher SSTs reported in 2010, favoring more storage of water vapor in the lower atmosphere. Therefore, the result implies that the warmer environment, with large transport of moisture, will generate a region with higher water vapor content, leading to higher volumes of rainfall. Thus the simulations with the warmer SSTs favored higher precipitation, which leads to significant increases in risks of extreme eventsin the ENEB region.

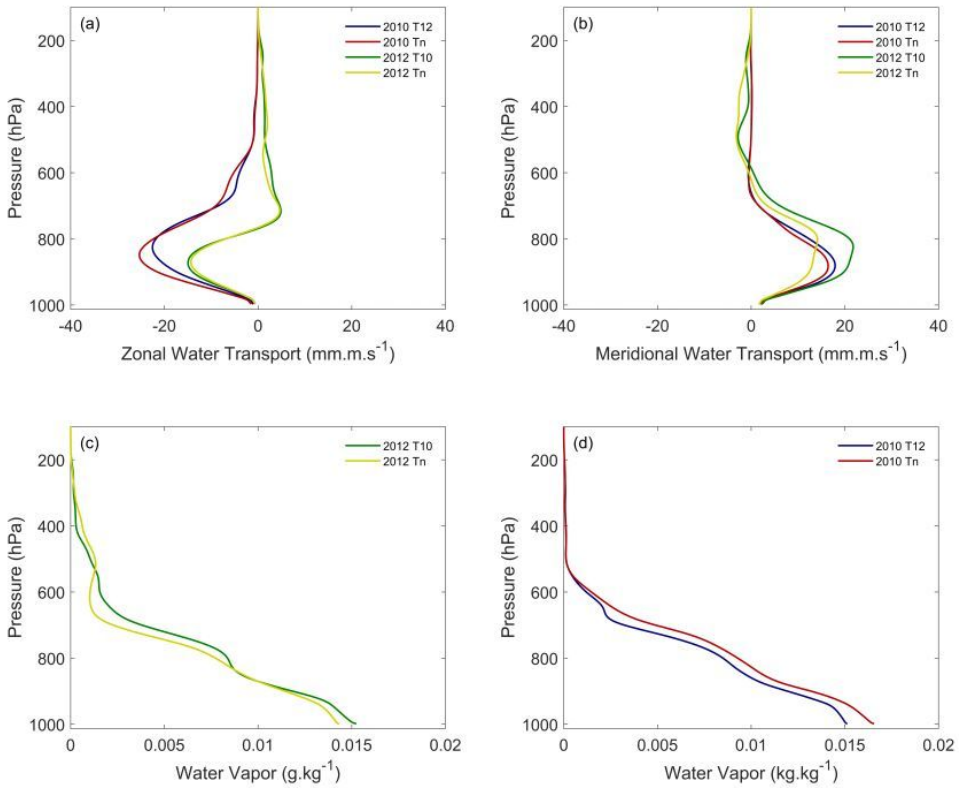

FIG. 13. Vertical profile of Zonal Water Vapor transport over peak activity region of weather event (a) and Vertical profile of Meridional Water Vapor Transport; Vertical profile of Water Vapor content for 2012 events (c) and for 2010 (d). The period of simulations is for June 2010 and 14 June 2012. The experiments is atmosphere for 2010 with SST with 2012 (blue); atmosphere for 2010 and SST for 2010 (red); atmosphere for 2012 and SST for 2010 (green); atmosphere for 2012 and SST for 2012 (yellow).

The simulations for accumulated rainfall (Figure 14) during the day of the event showed that the SST of 2010 contributed to intensify the total precipitation. In contrast, the SST of 2012 inhibited significant accumulated rainfall during the events. As a result, the influences of the SAWP simulated with the 2010 SST conditions indicate that even meteorological systems with the weak potential to cause heavy rainfall, such as the 2012 event, may lead to urban and social adversities. The SAWP SST played a crucial role in intensifying pre-existing weather systems. However, studies like those of Gomes et al. (2015) and Silva et al. (2018) showed that SST does not directly cause meteorological systems, which shows the non-linearity of SST on the formation of disturbances, although it intensifies those extreme rainfall events.

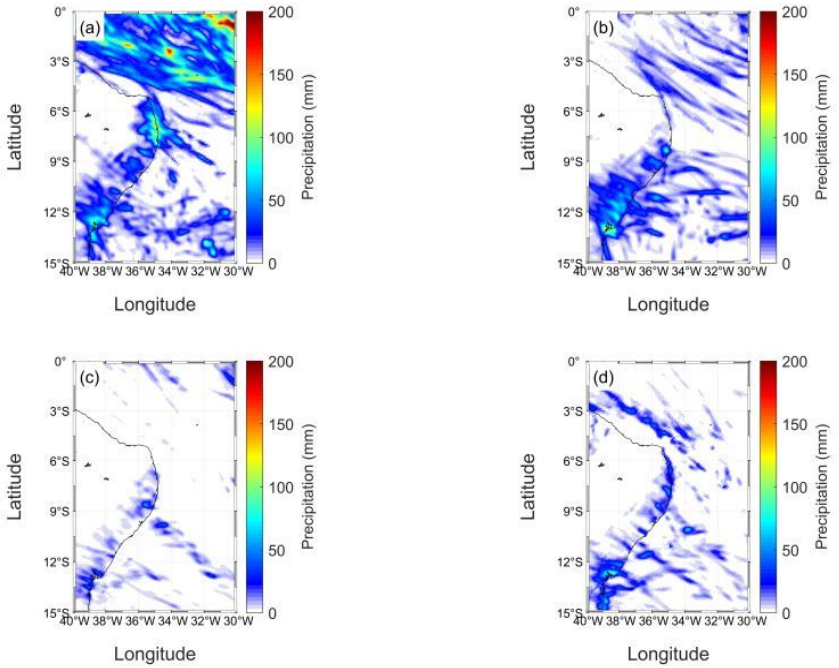

FIG. 14. Accumulated rainfall (mm) simulation during events: (a) June 17 and 18, 2010 with SST of the period. (b) June 17 and 18, 2010 with SST 2012. (c) June 14 and 15, 2012 with SST 2010. (d) June 14 and 15, 2012 with SST 2012.

The results show that the heat and humidity losses to the atmosphere were larger when there were higher SSTs. However, the loss of temperature from the ocean to the atmosphere was faster in the 2012 run with 2010 SSTs. It indicated that the atmosphere in 2012 favored a stronger cooling of the surface ocean waters, while in 2010 the temperature loss was weaker, which shows that the maintenance of high SST anomalies in 2010 was due to the air-sea dynamics as suggested by (Wang and Enfield 2003; Clement et al. 2005).

In addition, the lower surface pressure was associated with a higher SST, agreeing with Wang and Enfield (2001). The high SAWP SST values also favored a warmer atmosphere over ENEB coast than those with colder SST. Also, the SST changes directly influenced the lower layers of the atmosphere, increasing the vertical velocity. The 2012 omega with the 2010 SSTs showed a higher upward velocity compared to the 2012 run with 2012 SSTs, including upward movement throughout the atmosphere. In the 2010 run with 2012 SSTs, the upward velocity decreased, reducing the deep convection.

The results confirm the presence of higher instabilities when SAWP is present. It suggests that the oceanic waters in the SAWP region are dominant drivers in the intensification of the meteorological phenomena over the ENEB. The results also suggest that SAWP acted similar to other warm pools in other oceanic regions, as shown in works such as Brown and Zhang (1997), Wang and Enfield (2001, 2003), Wang et al. (2006) and Wang and Lee (2007). The increase in SST favored the warming of the atmosphere at low levels by the sensible and latent heat fluxes, increasing the vertical motion, and increasing the instability of the atmosphere.

d. Projections

Episodes of intense rainfalls and environmental disasters has already been registered in ENEB, such as the days (04-13-2020) in Salvador, (02-06-2020) in Sergipe, (02-12-2020) in Maceió, (04-24-2020) in Recife, (02-13-2020) in João Pessoa and (01-09-2020) in Natal, which caused transport, health, human, economic, and social security problems. The results obtained in this work and others (Debortoli et al. 2017; Rodrigues et al. 2020) show that the climate for ENEB is in warning pathways, with more intense precipitations in highly vulnerable urban sites, leading to more constant social impacts cases.

The assessment of SAWP SSTs impacts on the extreme rainfall events on ENEB is a crucial factor to future decision-making policies in mitigating vulnerabilities to climate change. Even though the region is a narrow coastal strip, the number of inhabitants sheltered in this region is high. In fact, the total of the metropolitan regions of the ENEB combined is close to 13.1 million, which corresponds to approximately 25% of the total population of NEB (IGBE, 2019).

Climate projections expect a substantial increase in ocean temperatures in the SAWP region. In fact, the SST over Atlantic regions shows that SAWP only occurs in a short period between February and April, or when positive anomalies are higher, reaching from January to May, and with the decrease starting from late May. However, the climate projections show that SAWP regions are shifted from being a possible appearance, to become a constant presence in the near-future scenario, and usual act in a long-future scenario.

As shown in previous results, the SAWP region leads to an increase in convective activity over the east coast of the NEB. Even when the synoptic conditions are not favorable to precipitation, as in 2012, positive SST anomalies in the SAWP region results in rainfall increase over the ENEB. Negative anomalies simulated a reduction in the total precipitation.

Therefore, it might be expected an increase in dynamical behavior that implies in a high amount of rainfall intensity. However, the results found in CPC Global Daily Unified Gauge-Based Analysis of Precipitation and measured data trends also show an increase in days without rain. This result is also worrisome due to the hydrological cycle in populous regions. The water supply in the metropolises may be impaired due to increased population and decreased total accumulated rainfall.

The relationship found in the COAWST simulation results, between SAWP SST and extreme rainfall over the ENEB, shows a higher potential virtual temperature, higher omega and stronger latent and sensible heat loss to the atmosphere. The key factor for increasing probability for an extreme rainfall event is the capability of the atmosphere in retaining more water vapor in a warmer environment, which can be represented by the potential virtual temperature. Furthermore, the positive feedback effects can contribute to the warming of the SAWP and the deepening of the ocean's surface layers, also increasing the amount of heat from the ocean's surface in these areas.

The air-sea thermodynamics also explains that the more significant warming of the atmosphere, a high amount of water vapor near the surface, and the decrease in surface wind speed, may inhibit the loss of sensible and latent heat fluxes. During periods when ocean-atmosphere temperature gradient are small, sensible and latent heat fluxes decrease causes an increase in SAWP SST. However, when gradient becomes higher, implying in a higher latent and sensitive heat loss, which is most present in projected scenarios than in the current patterns, it suggests more activity of SAWP for the ENEB rainfalls.

Moreover, climate models coarser resolutions could lead to a miss characterization of the future rainfall climatology in the east of the Brazilian northeast, essentially by the ENEB held in a narrow coastal strip with strong oceanic influence in the rains. Also, the general meteorological systems in the rainy season, as for example the easterlies wave disturbances showed in this work, are phenomena with a mesoscale extension which could be not well resolved with climate models with coarse resolutions. Finally, we suggest for future work a dynamical downscaling of climate models to understand the dynamical impact of climate projections scenarios in a high-resolution overview.

4 Conclusion

This work evaluates the 2010 and 2012 rainfall events in the ENEB under different SST anomalies over the South Atlantic Warm Pool region. Through air-sea coupled simulations and climate projection scenarios, it was possible to quantify the anomalous warm SST role during two events and under climate change scenarios.

This work reveals a shift in rainfall regime climatology at the eastern part of the Brazilian Northeast, characterized by an increase in days without rainfall and the frequency of intense precipitation above 100 mm.day-1. At the same time, there is a decrease in weak rainfall < 30 mm.day-1 occurrence. The atmospheric instabilities at the ENEB, consequently the extreme rainfall are forced by the positive anomalous SAWP temperature.

Moreover, this study indicates that the SAWP temperature significantly influences the instability of meteorological systems in the ENEB. The impacts were more significant in the lower atmosphere, especially in the variables that lead to low-level instabilities. Also, the atmospheric conditions favor the ocean environment to keep warmer, retaining the unstable conditions over the SAWP. The COAWST coupled-model simulations

evidence that meteorological events that present a small potential for rainfall events, as in 2012, can cause extreme rainfall events when combined with anomalous warming conditions of the SAWP, due to this instability potential induced by this region.

Climate projections indicate warm trends over the SAWP region. According to CMPI5 and CMPI6, this warming can lead from a condition of probable SAWP formation observed today to a state of permanent SAWP from 2070 to 2100, considering the models projected the "middle-of-road".

The climate variability in Brazilian Northeastern is strongly related to anomalies in the Pacific and Atlantic oceans. Further, 25% (about 13.5 million) of the population of this region are at the state capitals in the ENEB, which also presents high social inequality and susceptibility to natural disasters, such as flash floods, landslides, and sea-level rise. Therefore, it is essential to evaluate the climate change impacts concerning atmospheric events occurring in the entire Brazilian Northeast. Due to the ENEB inherent vulnerabilities, we highlight that it is crucial to formulate and guarantee public policy to deal with the impacts of these extreme events in this area, especially under this climate change scenario, as indicate the future projections for this region.

Acknowledgements

Author: The research leading to these results has received funding from the European Union's Horizon 2020 Programme (2014–2020) and from Brazilian Ministry of Science, Technology and Innovation through *Rede Nacional de Ensino e Pesquisa* (RNP) under the HPC4E project (http://www.hpc4e.eu), Grant Agreement 689772. This work is a contribution to the Brazilian Research Network on Global Climate Changes – Rede CLIMA (FINEP Grants 01.13.0353-00) and, to the TRIATLAS project, which has received funding from the European Union's Horizon 2020 research and innovation program under grant agreement No 817578. The first author thanks the Pernambuco Water and Climate Agency (APAC) for its research encourage. All group thanks for CPC Global Unified Precipitation data provided by the NOAA/OAR/ESRL PSL, Boulder, Colorado, USA, from their Web site at https://psl.noaa.gov/data/gridded/data.cpc.globalprecip.html. We acknowledge the World Climate Research Programme, which, through its Working Group on Coupled Modeling, coordinated and promoted CMIP5 and CMIP6. We thank the climate modeling groups for producing and making available their model output, the Earth System Grid Federation (ESGF) for archiving the data and providing access, and the multiple funding agencies who support CMIP5/CMIP6 and ESGF. P.T would like to thank the Foundation for the Support of Science and Technology of the State of Pernambuco - FACEPE, for the granting of the researcher scholarship.

Declarations

Funding: The research leading to these results has received funding from the European Union's Horizon 2020 Programme (2014–2020) and from Brazilian Ministry of Science, Technology and Innovation through *Rede Nacional de Ensino e Pesquisa* (RNP) under the HPC4E project (http://www.hpc4e.eu), Grant Agreement 689772.

Conflicts of interest/Competing interests: The received funding did not lead to any conflict of interests regarding the publication of this manuscript.

Availability of data and material: The data used in this research are freely accessible.

Code availability : The code used in this research will be available on request to the corresponding author.

Authors' contributions : TS and DV conceived the idea. AC, CP, RCMA, PT, FL, and LA performed the data acquisition and analysis, and all authors contributed extensively to the interpretation and analysis of the results, and the production of the final manuscript.

Ethics approval : Not applied.

Consent to participate: Not applied.

Consent to publication: All the authors have consented to publish this research.

References

Alves LM, Chadwick R, Moise A, et al (2021) Assessment of rainfall variability and future change in Brazil across multiple timescales. Int J Climatol 41:E1875–E1888. https://doi.org/10.1002/joc.6818

Andreoli RV, Kayano MT (2006) Tropical pacific and south atlantic effects on rainfall variability over northeast brazil. Int J Climatol 26:1895–1912. https://doi.org/10.1002/joc.1341

Andreoli RV, Kayano MT (2007) A importância relativa do atlântico tropical sul e pacífico leste na variabilidade de precipitação do Nordeste do Brasil. Rev Bras Meteorol 22:63–74. https://doi.org/10.1590/S0102-77862007000100007

Aragão JOR de (1998) O Impacto do ENSO e do Dipolo do Atlântico no nordeste do Brasil. Bull I'Institut français d'études Andin 27:839–844

Bojinski S, Verstraete M, Peterson TC, et al (2014) The concept of essential climate variables in support of climate research, applications, and policy. Bull Am Meteorol Soc 95:1431–1443. https://doi.org/10.1175/BAMS-D-13-00047.1

Bourras D, Reverdin G, Giordani H, Caniaux G (2004) Response of the atmospheric boundary layer to a mesoscale oceanic eddy in the northeast Atlantic. J Geophys Res Atmos 109:18114. https://doi.org/10.1029/2004JD004799

Brown RG, Zhang C (1997) Variability of Midtropospheric Moisture and Its Effect on Cloud-Top Height Distribution during TOGA COARE*. J Atmos Sci 54:2760–2774. https://doi.org/10.1175/1520-0469(1997)054<2760:VOMMAI>2.0.CO;2

Carvalho AA De, Montenegro AADA, Silva HP, Lopes I (2020) Trends of rainfall and temperature in Northeast Brazil Tendências da precipitação pluvial e da temperatura no Nordeste brasileiro. Rev Bras Eng Agrícola e Ambient 15–23

Cavalcanti EP, Gandu AW, Azevedo PVDE (2002) Transporte e balanço de vapor d'água atmosférico sobre o nordeste do brasil. Rev Bras Meteorol 17:207–217

Chelton DE, Xie S-P (2010) Coupled Ocean-Atmosphere Interaction at Oceanic Mesoscales. Oceanogr. Mag. 23:52–69

Cintra MM, Lentini CAD, Servain J, et al (2015) Physical processes that drive the seasonal evolution of the Southwestern Tropical Atlantic Warm Pool. Dyn Atmos Ocean 72:1–11. https://doi.org/10.1016/j.dynatmoce.2015.08.001

Clement AC, Seager R, Murtugudde R (2005) Why are there tropical warm pools? J Clim 18:5294–5311. https://doi.org/10.1175/JCLI3582.1

Costa MBSF, Mallmann DLB, Pontes PM, Araujo M (2010) Vulnerability and impacts related to the rising sea level in the Metropolitan Center of Recife, Northeast Brazil. Panam J Aquat Sci 5:169–177

Debortoli NS, Camarinha PIM, Marengo JA, Rodrigues RR (2017) An index of Brazil's vulnerability to expected increases in natural flash flooding and landslide disasters in the context of climate change. Nat Hazards 86:557–582. https://doi.org/10.1007/s11069-016-2705-2

Dos Santos CL, Listo FDLR, Da Silva OG, Dos Reis RB (2018) Análise metodológica de estudos referentes a eventos de movimentos de massa e erosão ocorridos na região Nordeste do Brasil / A methodological analysis of studies regarding events of mass and erosion movements occurring in the northeast region of Brazil. Cad Geogr 28:959–979. https://doi.org/10.5752/p.2318-2962.2018v28n55p959-979

Ebi KL, Nealon J (2016) Dengue in a changing climate. Environ Res 151:115–123. https://doi.org/10.1016/j.envres.2016.07.026

Fereira AG, Melo NGDS (2005) Principais sistemas atmosféricos atuantes sobre a região Nordeste do Brasil e a influência dos Oceanos. Rev Bras Climatol 1:15–28. https://doi.org/10.5380/abclima.v1i1.25215

Foltz GR, McPhaden MJ (2006) The role of oceanic heat advection in the evolution of tropical North and South Atlantic SST anomalies. J Clim 19:6122–6138. https://doi.org/10.1175/JCLI3961.1

Gomes HB, Ambrizzi T, Herdies DL, et al (2015) Easterly Wave Disturbances over Northeast Brazil: An Observational Analysis. Adv Meteorol 2015:1–20. https://doi.org/10.1155/2015/176238

Gomes JH, Silva TL do V, Guerra ER, Dias DT (2012) Ocupação em Área de Risco de Deslizamentos no Córrego do Jenipapo, Recife, Pernambuco. Rev Bras Geogr Física 03:524–539

Hänsel S, Medeiros DM, Matschullat J, et al (2016) Assessing Homogeneity and Climate Variability of Temperature and Precipitation Series in the Capitals of North-Eastern Brazil. Front Earth Sci 4:1–21. https://doi.org/10.3389/feart.2016.00029

Hastenrath S (2012) Exploring the climate problems of Brazil's Nordeste: A review. Clim Change 112:243–251. https://doi.org/10.1007/s10584-011-0227-1

Hounsou-gbo GA, Araujo M, Bourlès B, et al (2015) Tropical Atlantic Contributions to Strong Rainfall Variability Along the Northeast Brazilian Coast. Adv Meteorol 2015:13. https://doi.org/10.1155/2015/902084

Huang B, Thorne PW, Banzon VF, et al (2017) Extended reconstructed Sea surface temperature, Version 5 (ERSSTv5): Upgrades, validations, and intercomparisons. J Clim 30:8179–8205. https://doi.org/10.1175/JCLI-D-16-0836.1

Kouadio YK, Servain J, Machado LAT, Lentini CAD (2012) Heavy Rainfall Episodes in the Eastern Northeast Brazil Linked to Large-Scale Ocean-Atmosphere Conditions in the Tropical Atlantic. Adv Meteorol 2012:1–16. https://doi.org/10.1155/2012/369567

Liu C, Zipser EJ (2009) "Warm rain" in the tropics: Seasonal and regional distributions based on 9 yr of TRMM data. J Clim 22:767–779. https://doi.org/10.1175/2008JCLI2641.1

Marengo JA, Alves LM, Alvala RC, et al (2017) Climatic characteristics of the 2010-2016 drought in the semiarid Northeast Brazil region. An Acad Bras Cienc 1–13. https://doi.org/10.1590/0001-3765201720170206

Moscati MC de L, Gan MA (2007) Rainfall variability in the rainy season of semiarid zone of northeast Brazil (NEB) and its relation to wind regime. Int J Climatol 27:493–512. https://doi.org/10.1002/joc.1408

Moura AD, Shukla J (1981) On the dynamics of droughts in Northeast Brazil: Observations, theory, and numerical experiments with a general circulation model. J Atmos Sci 38:2653–2675. https://doi.org/10.1175/1520-0469(1981)038<2653:OTDODI>2.0.CO;2

Moura GB de A, Aragão JOR de, Melo JSP De, et al (2009) Relação entre a precipitação do leste do Nordeste do Brasil e a temperatura dos oceanos. Rev Bras Eng Agrícola e Ambient 13:462–469. https://doi.org/10.1590/S1415-43662009000400014

Moura GB de A, Brito JIB de, Sousa F de AS de, et al (2020) Revista Brasileira De Geografia Física. Rev Bras Geogr Física 13, n.04:1463–1482

Ncep (2000) NCEP FNL Operational Model Global Tropospheric Analyses, continuing from July 1999

Neves D, Alcântara CR, Souza EP De (2016) Estudo de Caso de um Distúrbio Ondulatório de Leste sobre o Estado do Rio Grande do Norte - Brasil Case Study of an Easterly Wave Disturbance Over Rio Grande do Norte State - Brazil. 490–505

Paegle JN, Mo KC (2002) Linkages between Summer Rainfall Variability over South America and Sea Surface Temperature Anomalies. J Clim 15:1389–1407. https://doi.org/10.1175/1520-0442(2002)015<1389:LBSRVO>2.0.CO;2

Peng S, Zhu Y, Huang K, et al (2016) Detecting the structure of marine atmospheric boundary layer over the Northern South China Sea by shipboard GPS sondes. Atmos Sci Lett 17:564–568. https://doi.org/10.1002/asl.693

Ramos RPL (1975) Precipitation characteristics in the Northeast Brazil dry region. J Geophys Res 80:1665–1678. https://doi.org/10.1029/JC080i012p01665

Rao VB, Lima MC, Franchito SH (1993) Seasonal and Interannual Variations of Rainfall over Eastern Northeast Brazil. J Clim 6:1754–1763. https://doi.org/10.1175/1520-0442(1993)006<1754:SAIVOR>2.0.CO;2

Renault L, Chiggiato J, Warner JC, et al (2012) Coupled atmosphere-ocean-wave simulations of a storm event over the Gulf of Lion and Balearic Sea. J Geophys Res Ocean 117:1–25. https://doi.org/10.1029/2012JC007924

Rodrigues DT, Gonçalves WA, Spyrides MHC, et al (2020) Spatial distribution of the level of return of extreme precipitation events in Northeast Brazil. Int J Climatol 40:5098–5113. https://doi.org/10.1002/joc.6507

Rodrigues RR, Haarsma RJ, Campos EJD, Ambrizzi T (2011) The impacts of inter-El Niño variability on the tropical Atlantic and northeast Brazil climate. J Clim 24:3402–3422. https://doi.org/10.1175/2011JCLI3983.1

Silva TL do V, Guedes RVS (2012) Análise do Comportamento Atmosférico em Situação de Seca: Uma abordagem Operacional para Pernambuco. Rev Bras Geogr Física 04:937–950

Silva TL do V, Veleda D, Araujo M, Tyaquiçã P (2018) Ocean-atmosphere feedback during extreme rainfall events in eastern Northeast Brazil. J Appl Meteorol Climatol 57:1211–1229. https://doi.org/10.1175/JAMC-D-17-0232.1

Torres RR, Ferreira NJ (2011) Case Studies of Easterly Wave Disturbances over Northeast Brazil Using the Eta Model. Weather Forecast 26:225–235. https://doi.org/10.1175/2010WAF2222425.1

Wallcraft AJ, Kara AB, Hurlburt HE, et al (2008) Value of bulk heat flux parameterizations for ocean SST prediction. J Mar Syst 74:241–258. https://doi.org/10.1016/j.jmarsys.2008.01.009

Wang C, Enfield DB (2003) A Further Study of the Tropical Western Hemisphere Warm Pool. Phys Oceanogr 16:1476–1493. https://doi.org/http://dx.doi.org/10.1175/1520-0442-16.10.1476

Wang C, Enfield DB (2001) The tropical Western Hemisphere warm pool. Geophys Res Lett 28:1635–1638. https://doi.org/10.1029/2000GL011763

Wang C, Enfield DB, Lee SK, Landsea CW (2006) Influences of the Atlantic warm pool on western hemisphere summer rainfall and Atlantic hurricanes. J Clim 19:3011–3028. https://doi.org/10.1175/JCLI3770.1

Wang C, Lee SK (2007) Atlantic warm pool, Caribbean low-level jet, and their potential impact on Atlantic hurricanes. Geophys Res Lett 34:1–5. https://doi.org/10.1029/2006GL028579

Warner JC, Armstrong B, He R, Zambon JB (2010) Development of a Coupled Ocean–Atmosphere–Wave–Sediment Transport (COAWST) Modeling System. Ocean Model 35:230–244. https://doi.org/10.1016/j.ocemod.2010.07.010

Warner JC, Perlin N, Skyllingstad ED (2008) Using the Model Coupling Toolkit to couple earth system models. Environ Model Softw 23:1240–1249. https://doi.org/10.1016/j.envsoft.2008.03.002

Xie P, Yatagai A, Chen M, et al (2007) A gauge-based analysis of daily precipitation over East Asia. J Hydrometeorol 8:607–626. https://doi.org/10.1175/JHM583.1

Zeng XB, Brunke MA, Zhou MY, et al (2004) Marine Atmospheric Boundary Layer Height over the Eastern Pacific : Data Analysis and Model Evaluation. J Clim 17:4159–4170. https://doi.org/10.1175/JCLI3190.1